Archival Report

Biological Psychiatry: GOS

Electroencephalography Biomarkers of α5-GABA Positive Allosteric Modulators in Rodents

Frank Mazza, Alexandre Guet-McCreight, Thomas D. Prevot, Taufik Valiante, Etienne Sibille, and Etay Hay

ABSTRACT

BACKGROUND: Reduced cortical inhibition mediated by GABA (gamma-aminobutyric acid) is reported in depression, anxiety disorders, and aging. A novel positive allosteric modulator that specifically targets the α5-$GABA_A$ receptor subunit (α5-PAM), ligand GL-II-73 shows anxiolytic, antidepressant, and procognitive effects without the common side effects associated with nonspecific modulation by benzodiazepines such as diazepam, thus suggesting novel therapeutic potential. However, it is unknown whether α5-PAM has detectable signatures in clinically relevant brain electroencephalography (EEG).

METHODS: We analyzed EEG in 10 freely moving rats at baseline and following injections of α5-PAM (GL-II-73) and diazepam.

RESULTS: We showed that α5-PAM specifically decreased theta peak power, whereas diazepam shifted peak power from high to low theta while increasing beta and gamma power. EEG decomposition showed that these effects were periodic and corresponded to changes in theta oscillation event duration.

CONCLUSIONS: Thus, our study shows that α5-PAM has robust and distinct EEG biomarkers in rodents, indicating that EEG could enable noninvasive monitoring of α5-PAM treatment efficacy.

https://doi.org/10.1016/j.bpsgos.2024.100435

Cortical inhibition mediated by GABA (gamma-aminobutyric acid) is reduced in depression (1,2), anxiety disorders (3), aging (4), and neurodegenerative disorders (5). Accordingly, nonspecific $GABA_A$ receptor positive allosteric modulators (PAMs) in the benzodiazepine drug class, such as diazepam (DZP), have been used as common pharmacological treatments (6). However, nonspecific potentiation by DZP leads to side effects, such as amnesia and sedation, thereby limiting their therapeutic potential (7). In contrast, studies of chronically stressed rats, which exhibit many symptoms of depression, showed that a novel α5-$GABA_A$ receptor subunit PAM (α5-PAM), ligand GL-II-73, has anxiolytic, antidepressant, and procognitive effects without the common side effects associated with DZP, thus suggesting novel therapeutic potential for depression and aging (8–13). The anxiolytic potential of GL-II-73 and other α5-PAMs has also been shown in nonstress conditions (8) in nonstressed old mice (13) and nonstressed transgenic mice (11). However, quantitative in vivo measures of drug effects are needed for both development and clinical translation. Electroencephalography (EEG) offers a noninvasive and cost-effective method to monitor brain activity and treatment response, but it remains unknown whether α5-PAM effects exhibit distinct EEG biomarkers.

$GABA_A$ receptors are a key component by which GABA exerts its inhibitory effect, whereby subunit composition determines channel localization and properties (14–16). Whereas the α1 subunit is widely distributed across neuron and interneuron types and throughout the brain (17–19), α5 subunits are primarily expressed in the apical dendrites of pyramidal neurons and mainly in the hippocampus (20,21) and neocortex (16). α5-$GABA_A$ receptors mediate lateral inhibition to pyramidal neurons by somatostatin (SST)-expressing interneurons that target the apical dendrites (18,22,23). Reduced α5-$GABA_A$ receptors may underlie deficits in GABAergic and SST signaling, which have been identified as contributors to preclinical models of depression and cognitive impairment (24,25) and supported by computational models (26,27). α5 Subunit knockout mice exhibit altered phasic and tonic currents, as well as cognitive changes including altered memory, executive function, and fear conditioning (28–30). Relatedly, silencing SST interneuron inhibition leads to depression symptoms in preclinical rodent models (31), which are reversed by α5-$GABA_A$ receptor PAMs (8,31).

α5-PAMs may have clear and distinct signatures in EEG due to their strong inhibitory modulation of the apical dendrites of L2/3 and L5 pyramidal neurons, which are the main contributors of the EEG dipole, thus offering a powerful tool for noninvasive treatment monitoring (32). Previous studies with rodents have extensively characterized the effects of benzodiazepines, which predominantly reduced cortical theta (4–8 Hz) and increased beta (12–30 Hz) oscillation frequency in a behavior-dependent manner without affecting total cortical or hippocampal theta power (33). Previous rat task studies have shown that EEG beta and gamma (30–50 Hz) power are

ISSN: 2667-1743

uniquely elevated by $GABA_A$ receptor α2/3-potentiating drugs, such as benzodiazepines (33). It remains to be determined whether α5-PAM displays EEG signatures that are distinct from those of DZP, such as involving power in theta band. Studies have shown that hippocampal SST interneuron stimulation slows theta oscillations in rodents (34), and reduced SST inhibition decreases theta power in computational studies of detailed human cortical microcircuits (27). Furthermore, α5 subunit knockout mice show reduced hippocampal-dependent fear-associated learning specifically during theta stimulation, which are oscillations that are modulated by SST interneurons (35–38).

In this study, we measured EEG in freely moving rats that were administered α5-PAM ligand GL-II-73, henceforth referred to as α5-PAM, which had previously been shown to have antidepressant, procognitive, and anxiolytic effects in chronically stressed mice (8). We compared the EEG effect with both vehicle and DZP and analyzed features of the EEG as putative biomarkers of α5-PAM compared with DZP. Then we decomposed the power spectral density (PSD) into aperiodic and periodic components to further differentiate EEG features following α5-PAM and DZP application. Finally, we compared the EEG features across different doses of each drug compared with doses that had previously been identified as optimal in preclinical mouse experiments (8).

METHODS AND MATERIALS

Animals

Sprague Dawley rats were provided by Charles River Laboratories (N = 10, age 7.3 ± 0.6 weeks, all male). The animal experiments, including EEG recordings, were performed at Charles River Laboratories. Eight rats were used at any given session of the study because 2 rats were substituted with rats of similar age due to tail lesions that were found during weeks 4 and 6 of the study. Rats were group housed in polycarbonate cages (2–3 per cage) and acclimated for at least 4 days in a 12-hour light/dark cycle with consistent room temperature (22 ± 2 °C), 50% humidity, food and water ad libitum, as well as a nylon bone (Bio-Serv, K3580) and tunnel retreat (Bio-Serv, K3245) for enrichment. Surgery was performed to implant electrodes for EEG recording (see below). All baseline and postinjection EEG recordings that were analyzed were taken during the light phase. Rat age was 10.1 ± 0.2 weeks when EEG recordings started. All experiments were conducted in accordance with protocols approved by the Institutional Animal Care and Use Committee of Charles River Laboratories SSF.

Surgery

EEG/electromyography (EMG) subcutaneous transmitters (model number: HD-S02) were obtained from Data Sciences International. Rats were anesthetized with isoflurane (2%, 800 mL/min O_2). Local anesthesia was provided with bupivacaine, and postoperative analgesia was provided with carprofen. The EEG transmitter was inserted into a pocket made close to the dorsal flank. Positive and negative leads were tunneled subcutaneously toward the head. The positive lead was placed 2 mm anterior from the bregma and 2 mm lateral from the midline (left frontal cortex). The negative lead was placed 2 mm anterior to the lambda and 2 mm lateral from the midline (right parietal cortex). To record EMG activity, the positive lead and negative leads were sutured on the left and right musculus cervicoauricularis. Following surgery, rats were individually housed in cages. They were provided food and water ad libitum, as well as a nylon bone (Bio-Serv, K3580) and paper towel for enrichment. Rats received a 5-day course of antibiotics immediately following surgery. Pain was managed for 3 days. EEG recording began after a minimum of 10 days of recovery following surgery.

Injected Ligands

Rats were tested with 1 of 6 injected ligands from 3 groups: control vehicle; α5-PAM (GL-II-73) of either 1, 3, or 10 mg/kg dose; and DZP of either 0.5 or 1 mg/kg dose (supplied by Sigma, Lot #105F0451, purity >99%). All ligands were held at room temperature. Ligands were formulated on days of use in a vehicle solution of 85% distilled H_2O, 14% propylene glycol, and 1% Tween-80 for vehicle and α5-PAM or 50% distilled H_2O, 40% propylene glycol, and 10% alcohol for DZP. The route of administration for all ligands was through intravenous tail vein.

Experimental Design

Rats were injected with 1 of 6 test ligands in a standard Latin-square design. Rats were placed on RPC-1 receivers the night prior to recording for acclimation. Rats were recorded weekly (at least 5 days between each session). Baseline recording began at approximately 9 AM. After approximately 1 hour, rats were injected with a test ligand. Recording continued for an additional 24 hours following injection. All rats were euthanized via CO_2 asphyxiation following experiment completion (week 6). Video was recorded during the entirety of baseline and treatment.

EEG Preprocessing

EEG and EMG data were downsampled to 140 Hz and visually inspected for artifacts. Active periods for each rat were identified after at least 3 seconds of continuous high-amplitude EMG data, excluding a 2-second buffer between active and other states (such as sleep). The continuous segments were treated as epoched data for PSD computation to ensure that there were no concatenation artifacts. Sixty minutes of baseline EEG and 50 to 70 minutes of postinjection data were included in the analysis because the rodent incidence of sleep increased 80 minutes post-DZP injection. There was no significant difference between conditions in the length of EEG data of active periods 50 to 70 minutes postinjection. In 6 of the 48 sessions, where no high-quality active-state EEG was found during this window, the window of inclusion was expanded to 30 to 70 minutes. The overall postprocessed EEG length used in the analysis was 15.2 minutes (95% CI, 1.8–43.2) for baseline and 4.6 minutes (95% CI, 0.1–14.0) for the postinjection EEG window. There was no significant difference in postinjection EEG length between conditions (ps > .23 for all). In 4 of 48 sessions, the EEG length was <1 minute, but it was sufficient to calculate the features of interest, and it did not deviate from the group statistics.

EEG Analyses

EEG PSD was calculated using Welch's method, with a 3-second Hanning window, median average, and 30% window overlap. We decomposed EEG PSDs into periodic and aperiodic components using FOOOF (39). The aperiodic component of the PSD was a 1/f function defined by a vertical offset and exponent parameter. After removing the aperiodic component from the PSDs, we derived the periodic components (representing putative oscillations) from the flattened spectrum using gaussians, which were defined by center frequency (mean), bandwidth (variance), and power (height). Power spectra were fit across the frequency range 1 to 70 Hz with a resolution of 0.33 Hz. Fitting algorithm settings were as follows: width limits = (1.5, 8); maximum number of peaks = 5; minimum peak height = 0.3; peak threshold = 3; and aperiodic mode = "fixed," where the aperiodic component was fit as a straight line to the PSD. Model fits were evaluated using FOOOF's built-in least squares evaluation method. Bootstrapped mean model fit error for all conditions were <0.2 for <30 Hz frequencies and did not differ significantly between models that were fit with or without a knee. Canonical EEG bands were identified as delta (1–4 Hz), theta (4–8 Hz), alpha (8–12 Hz), beta (12–30 Hz), and gamma (30–50 Hz). Groupwise differences across PSD curves were included in the analysis if a significant change in power was detected over a continuous span of 0.66 Hz.

EEG Theta Event Analysis

We analyzed characteristics of events of large amplitude in low theta (4–6 Hz) and high theta (6–8 Hz) to identify which aspect of EEG waveforms contributed to overall power changes in periodic theta. For each rodent, the threshold for a large-amplitude event was calculated by averaging the instantaneous envelope power (Hilbert transform) of baseline recordings. We calculated maximum envelope power and duration at sections for large-amplitude events. Event frequency was calculated as number of events per second. The same methodology was applied to 50- to 70-minute postinjection EEG, using the threshold established in the baseline EEG.

EEG Cycle-by-Cycle Analysis

We analyzed neural oscillations on a cycle-by-cycle basis using the python package *bycycle* (40). Using *bycycle's* standard analysis workflow, EEG time series were first low bandpass filtered at 30 Hz to limit high-frequency noise. Next, data were bandpass filtered for theta (3–9 Hz) to estimate zero-crossings as well as peaks and troughs corresponding to theta oscillations. Finally, midpoints between peaks and zero crossings were identified. Burst detection threshold parameters were as follows: amp_fraction (minimum relative amplitude) = 0.1, amp_consistency (relative difference between cycle rise and decay amplitude) = 0.5, period_consistency (relative distance between adjacent periods) = 0.5, monotonicity (consistency of rise and decay phases) = 0.6, and min_n_cycles (minimum number of consecutive cycles) = 3.

Inclusion/Exclusion Criteria

Two of the 48 recording sessions were removed from analysis because the EEG exhibited outlier behavior using the standard Q3 + 1.5 × interquartile range method referencing peak theta power.

Statistical Tests

To provide a more robust estimate of group differences despite the small sample size, a significant difference between 2 groups was determined by a 2-tailed test of their bootstrapped difference being different than 0 (10,000 bootstrap iterations). Between-group comparisons were achieved using the same method, and the Bonferroni method was used to correct for multiple comparisons.

RESULTS

Male Sprague Dawley rats (n = 8) were injected with either vehicle, α5-PAM GL-II-73, or DZP in a random Latin-square design, with at least 1 week between injections (Figure 1A). EEG and EMG were recorded at baseline and following intravenous injection using surgically implanted single-channel subcutaneous EEG and EMG sensors (Figure 1B, C). We analyzed active-state EEG by calculating the PSD. All baseline EEGs displayed a prominent theta peak (at 7.1 ± 0.4 Hz) and 1/f slope characteristic of wakefulness (41) (Figure 1D), with no presentation of characteristic of non–rapid eye movement or rapid eye movement sleep such as elevated delta or solely high theta (42).

We compared baseline and postinjection EEG for rats injected with vehicle, 3 mg/kg α5-PAM, and 1 mg/kg DZP. Whereas EEG did not change significantly postinjection of vehicle ($p > .05$) (Figure 2A), injection of α5-PAM decreased theta power around 7 Hz in the raw averaged PSD (−57%, $p < .05$, $d = -3.7$) (Figure 2B) and did not affect power in other averaged frequency bands (all ps $> .05$). In contrast, DZP injection shifted the theta peak from high theta to low theta (increasing power in 4.3–5.0 Hz and decreasing power in 6.0–9.3 Hz). DZP also increased beta power in 14 to 30 Hz (+121%, $p = .002$, $d = 1.7$) and increased gamma power in 30 to 44 Hz (+86%, $p = .002$, $d = 1.7$) (Figure 2C). The window of 50 to 70 minutes postinjection was chosen for analysis because it exhibited the largest and most consistent change in EEG spectrogram compared with baseline in all injections (Figure 2G–I).

To better differentiate EEG changes due to α5-PAM versus DZP, we decomposed the PSD into aperiodic and periodic components and compared changes in periodic theta features (peak power, bandwidth, center frequency). α5-PAM injection decreased periodic theta power (−24%, $p = .026$, $d = -1.1$) (Figure 2E) and slightly decreased the center frequency (−9%, $p = .002$, $d = -1.8$). In contrast, DZP did not significantly change periodic theta power (−6%, $p > .05$) (Figure 2F), but rather decreased bandwidth (−29%, $p < .001$, $d = -2.9$) and decreased center frequency (−18%, $p = .001$, $d = -2.0$), both to a larger extent than α5-PAM (bandwidth: −33%, $p = .003$, $d = 2.4$; center frequency: +14%, $p = .015$, $d = -1.4$). There were no significant changes in aperiodic component parameters, offset, or exponent for any conditions (all ps $> .05$) except for DZP, where injection reduced the aperiodic exponent (−15%, $p = .026$, $d = 1.2$). Vehicle injection did not affect periodic theta power, bandwidth, or center frequency (all ps $> .05$) (Figure 2D).

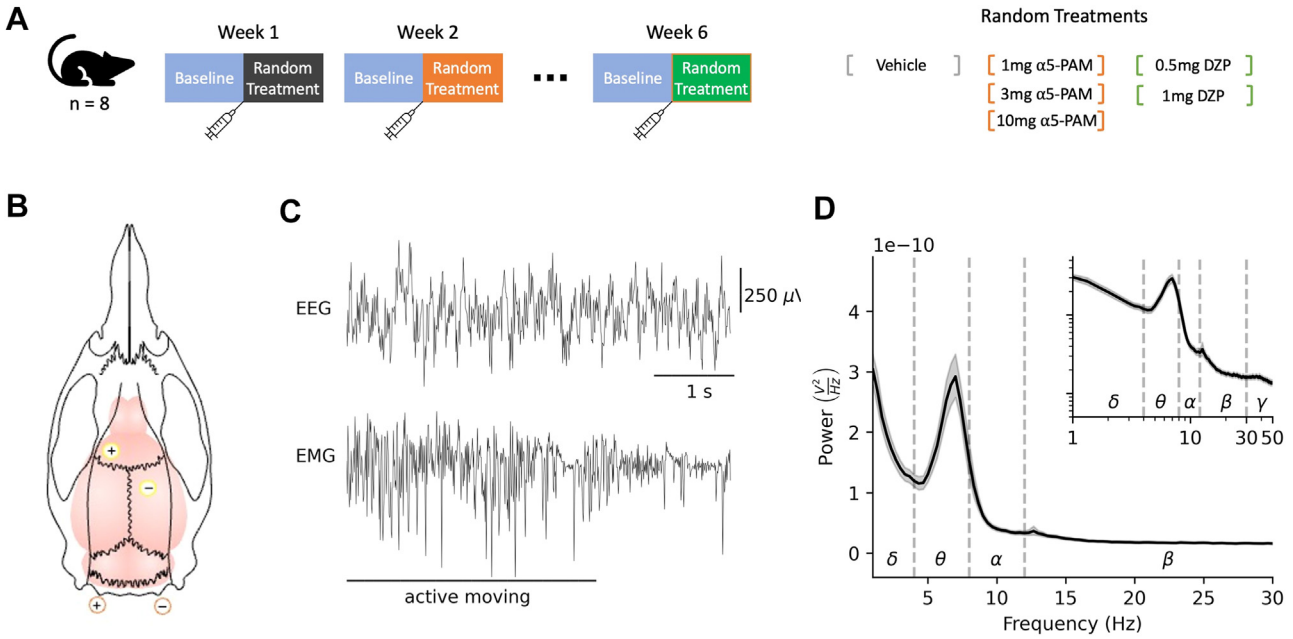

Figure 1. Testing α5-PAM and EEG recording in freely moving rats. **(A)** Experimental protocol, where EEG and EMG were recorded for 60 minutes at baseline (pre-injection) and 60 minutes following injection of a random intravenous treatment, either vehicle, 1 mg/kg α5-PAM, 3 mg/kg α5-PAM, 10 mg/kg α5-PAM, 0.5 mg/kg DZP, or 1 mg/kg DZP. Rats were freely moving during the session. A week interval separated each injection session so that at the end of 6 weeks, all types of injections had been administered. **(B)** Schematic showing subdural EEG electrode lead placement (yellow) and EMG electrode lead placement (orange). **(C)** Example of simultaneously recorded EEG and EMG while the rats were in active state. **(D)** Power spectral density plot of active-state EEG for baseline condition (n = 8 rats, bootstrapped mean and 95% CIs). Inset: same power spectral density plot shown on log-log scale. α5-PAM, α5-$GABA_A$ receptor subunit positive allosteric modulator; DZP, diazepam; EEG, electroencephalography; EMG, electromyography.

To characterize the dose-response effect of α5-PAM and DZP on EEG, we analyzed additional doses of each drug (1 and 10 mg/kg α5-PAM, as well as 0.5 mg/kg DZP). The low and high doses of α5-PAM did not significantly affect the PSD, in contrast to the 3 mg/kg α5-PAM dose (all ps $>$ .05) (Figure 3A, B, E, G), except that the 1 mg/kg dose of α5-PAM tended to increase bandwidth similarly to the 3 mg/kg dose (+13%, p = .05, d = 1) (Figure 3C). The lower dose of DZP showed a similar trend to 1 mg/kg DZP, although to a smaller extent, by decreasing theta bandwidth (−22%, p = .043, d = 1), a negligible decrease in center frequency (−7%, p = .1, d = 0.9), and no change in peak power (p > .05).

To determine the aspects of the EEG signal underlying the theta power modulation by the compounds, we detected low theta (4–6 Hz) and high theta (6–8 Hz) oscillatory events and compared their amplitude, frequency (events per second), and duration in rats at baseline and postinjection. α5-PAM decreased high-theta event duration compared with baseline (−12%, p = .01, d = −1.4) (Figure 4C) and increased event frequency (9%, p = .15, d = 1.3). DZP similarly decreased high theta event duration (−14%, p < .001, d = 1.8), but increased low theta event duration to a larger extent (28%, p < .001, d = 2.6). DZP also decreased low theta event frequency (−19%, p = .001, d = −3.7) (Figure 4D) and high theta event amplitude (−16%, p = .006, d = 1.4). Vehicle did not affect any of the EEG waveform components. Finally, we performed a complementary oscillatory cycle-by-cycle analysis of theta to limit a priori assumptions of bandwidth and possible narrowband filtering. α5-PAM reduced theta burstiness (−22%, p < .001, d = −2.3) (Figure 4G), whereas DZP increased theta oscillation amplitude (29%, p = .013, d = 1.7) (Figure 4E). DZP injection increased theta period (14%, p < .001, d = 2.4) (Figure 4F), which only slightly increased following α5-PAM injection (7%, p < .001, d = −2.2). Vehicle did not affect theta oscillations except for a slight increase in period (5%, p = .001, d = 1.8).

DISCUSSION

In this work, we identified in freely moving rats the EEG signatures of α5-PAM using GL-II-73, a ligand that has been shown to have therapeutic effects in chronically stressed mice in terms of mood and cognitive symptoms. We showed that α5-PAM had a distinct effect of decreasing peak theta power, whereas nonspecific modulation by DZP shifted peak power from high theta to low theta. EEG decomposition and event analysis showed that these effects were seen more strongly in the periodic component of the decomposed PSD, modulated by theta event amplitude and duration in DZP as opposed to specifically reduced high theta event duration in the α5-PAM. We characterized the dose-response effect of α5-PAM on EEG and found that the dose of 3 mg/kg had the largest specific effect on peak EEG power in the theta frequency band. Thus, our study demonstrates that subunit-specific potentiation of the α5-$GABA_A$ receptor has distinct signatures in rodent EEG, suggesting candidate biomarkers for efficacy and monitoring of α5-PAM treatment for depression in human subjects.

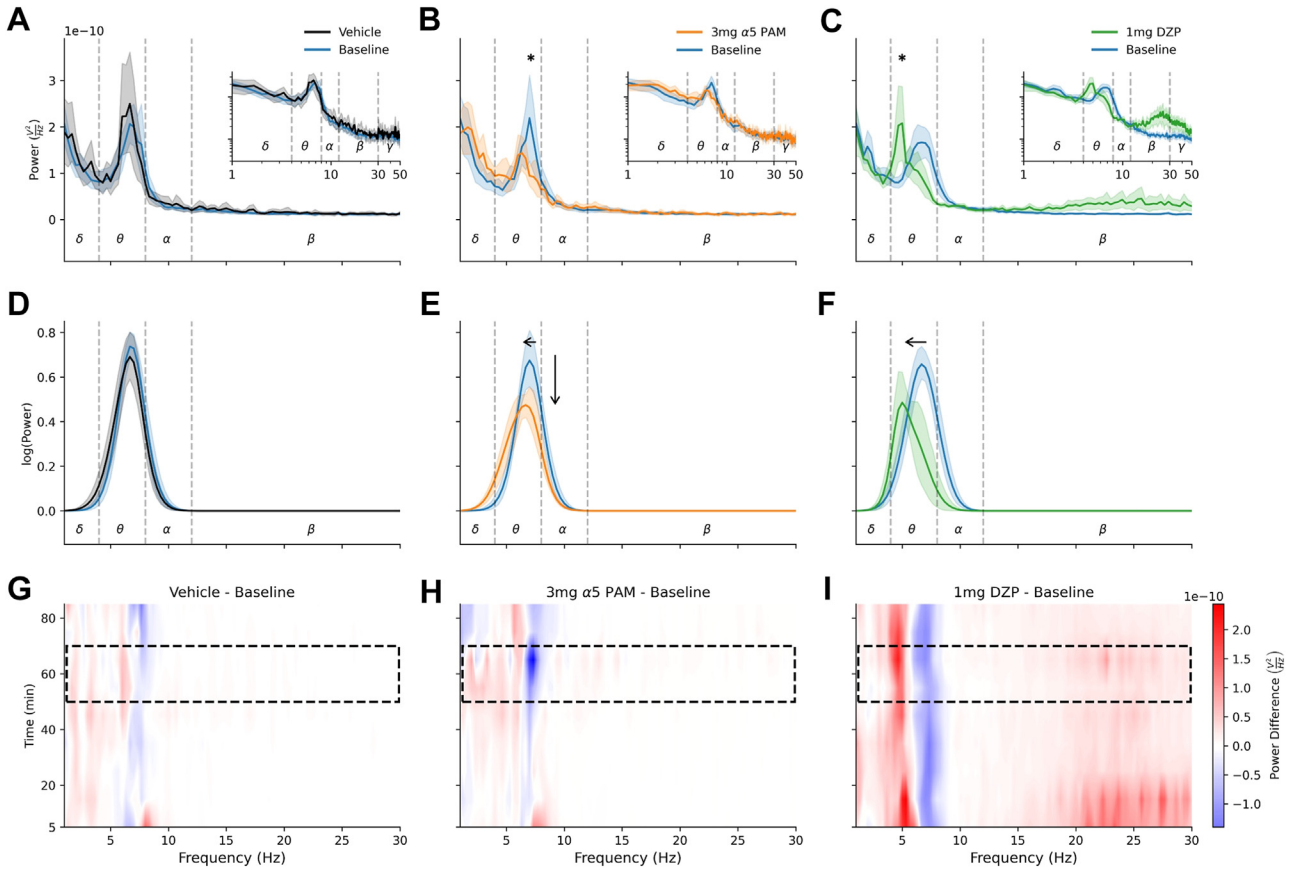

Figure 2. EEG signatures of α5-PAM in absolute and periodic component of PSD are specific from DZP. **(A)** PSD for active-state EEG recordings pre-injection (baseline, blue) and 50 to 70 minutes postinjection of vehicle [black, **(A)**], showing bootstrapped mean and 95% CIs. Inset: same PSD data shown on log-log scale. **(B)** PSD in the case of 3 mg/kg α5-PAM injection (orange) reduced peak theta power compared with baseline (blue). **(C)** PSD in the case of 1 mg/kg DZP injection (green) did not reduce the peak theta power but primarily left-shifted the peak and increased beta peak power. **(D)** Fitted periodic component for vehicle injection (black) and baseline (blue). **(E)** Fitted periodic component for 3 mg/kg α5-PAM injection (orange) and baseline (blue). **(F)** Fitted periodic component for 1 mg/kg DZP injection (green) compared with baseline (blue). **(G–I)** Spectrogram of difference from baseline in active-state EEG recordings 5 to 85 minutes postinjection of vehicle **(G)**, 3 mg/kg α5-PAM **(H)**, or 1 mg/kg DZP **(I)**. Dotted rectangle shows the window of 50 to 70 minutes used in postinjection PSD analysis for panels **(A–F)**. α5-PAM, α5-$GABA_A$ receptor subunit positive allosteric modulator; DZP, diazepam; EEG, electroencephalography; PSD, power spectral density.

The α5-PAM ligand GL-II-73, which was previously shown to have anxiolytic, antidepressant, and procognitive effects (8), primarily decreased EEG theta power in this study. This is consistent with the increased resting-state theta power that is often seen in patients with depression and that is correlated with depression severity (43,44). Increased theta power is also correlated with first-line treatment resistance and with second-line treatment response (43,45–50), especially with second-line treatments that target frontal cortical inhibition and decrease theta power following treatment (49,51–54). Increased theta power has also been associated with cognitive impairment (55), and increased theta coherence is associated with anxiety (56). The decreased theta effect by the α5-PAM ligand reported in this study suggests that the inhibitory mechanisms that it targets may underlie the EEG effects described above. This is supported by previous studies that have indicated that reduced SST interneuron inhibition [which targets α5-$GABA_A$ receptor (31)] in frontal regions is central to depression etiology (57–59) and studies that have shown that SST interneurons provide rhythmic theta inhibition (60). The link between reduced SST interneuron inhibition and theta power is further supported by detailed simulations of depression microcircuits showing that reduced SST interneuron inhibition primarily modulated theta power (27); by in vivo studies in the cortex and the hippocampus showing that theta oscillations are directly modulated by optogenetic stimulation of SST interneurons (34); and by optogenetic studies showing that inhibition of prefrontal SST interneurons affected local oscillations and long-range theta-mediated prefrontal-hippocampal synchrony (61). GL-II-73 reduced theta oscillations well within the canonical rodent theta frequency range (3–10 Hz) rather than higher frequencies (62,63). While SST inhibition may underlie theta changes in humans (27) and theta oscillations in rodents (64,65), future work should differentiate SST's role in modulating dominant alpha in humans versus dominant theta in rodents (62,63). Together, these previous studies and our current results

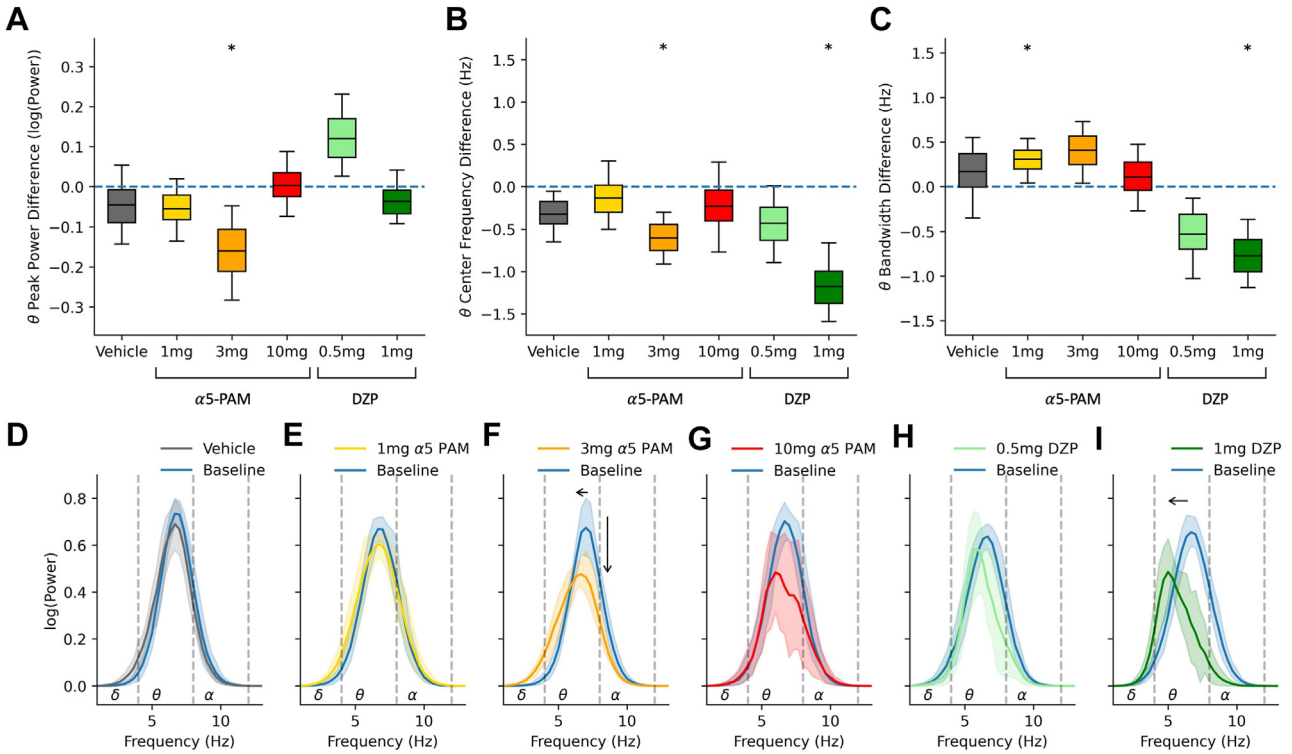

Figure 3. Electroencephalography signatures of different α5-PAM and DZP doses. **(A)** Periodic theta peak power (bootstrapped mean difference from baseline and 95% CI) for the different conditions. Asterisk shows significant difference between baseline and injection. **(B)** Same as panel **(A)** but for periodic theta center frequency. **(C)** Same as panel **(A)** but for periodic theta peak bandwidth. **(D–I)** Fitted periodic component of power spectral density preinjection for baseline (blue) and 50 to 70 minutes postinjection of **(D)** vehicle, **(E)** 1 mg/kg α5-PAM, **(F)** 3 mg/kg α5-PAM, **(G)** 10 mg/kg α5-PAM, **(H)** 0.5 mg/kg DZP, and **(I)** 1 mg/kg DZP. Showing bootstrapped mean and 95% CIs. The vertical arrow shows significant difference in theta power peak, and horizontal arrows show significant difference in theta power center frequency. α5-PAM, α5-$GABA_A$ receptor subunit positive allosteric modulator; DZP, diazepam.

indicate that the theta modulation that is relevant to depression and treatment is likely mediated through α5-$GABA_A$ receptor innervation by SST interneurons.

Although our study is the first to identify EEG biomarkers of α5-positive modulation, previous studies have identified EEG biomarkers of other $GABA_A$ receptors. For example, GABA α2/3 subunit potentiation has been shown to increase beta and gamma power, consistent with benzodiazepine changes seen in previous studies (66) and consistent with the DZP effects that we observed. Relatedly, zolpidem, which is a potentiator of α1, was shown to modulate cortical and hippocampal delta power (33). Specific α1 potentiation also increased delta and beta power in active rodents (67). Together, our findings further support that specific $GABA_A$ receptor subunit potentiation has signatures that are detectable in EEG. The robust EEG signatures of α5-$GABA_A$ receptor potentiation at the 3 mg/kg dose are likely due to α5 subunit mediating inhibition onto layer 2/3 and 5/6 pyramidal neurons, which are the primary contributors to EEG, and more specifically due to the location of α5-$GABA_A$ receptors on the apical dendrites, which strongly affect the EEG dipole (25,36). This is also supported by the U-shaped dose-response of the α5-PAM whereby the 1 mg/kg dose may not activate α5-$GABA_A$ receptors strongly enough, whereas the 10 mg/kg dose may lead to spillover potentiation of GABA α2/3 subunits (8), as indicated by an increase in beta power characteristic of benzodiazepine and GABA α2/3 subunit potentiation (66) that may also counter the reduced theta effect of the moderate α5-PAM dose.

We identified global changes in theta power as a biomarker of α5-PAM GL-II-73, which constitute promising preclinical EEG correlates for treatment monitoring. Because a bipolar montage was used, where the positive electrode was placed on top of the left frontal cortex and the negative reference electrode on top of the right parietal cortex, our results reflect changes in relative activity and thus potential between these 2 regions (68). Thus, the changes may reflect local increased frontal theta activity as seen in depression (46); altered communication between frontal and hippocampal regions, which is key for working memory (64,65); or a combination of the two. These possibilities are consistent with α5 subunits being abundantly expressed in rodent frontal and hippocampal regions, where they mediate SST interneuron inhibition (15). Future studies should include higher-density EEG recordings to identify location-specific changes and thus enhance the translation to human EEG. Relatedly, work to identify changes in theta power in other brain states will provide additional important biomarkers of α5 potentiation because SST interneuron inhibition has been shown to play a role at rest (69), during task (70), and during slow-wave sleep (71). Previous in vivo (34,38) and in silico (27) work showing that SST

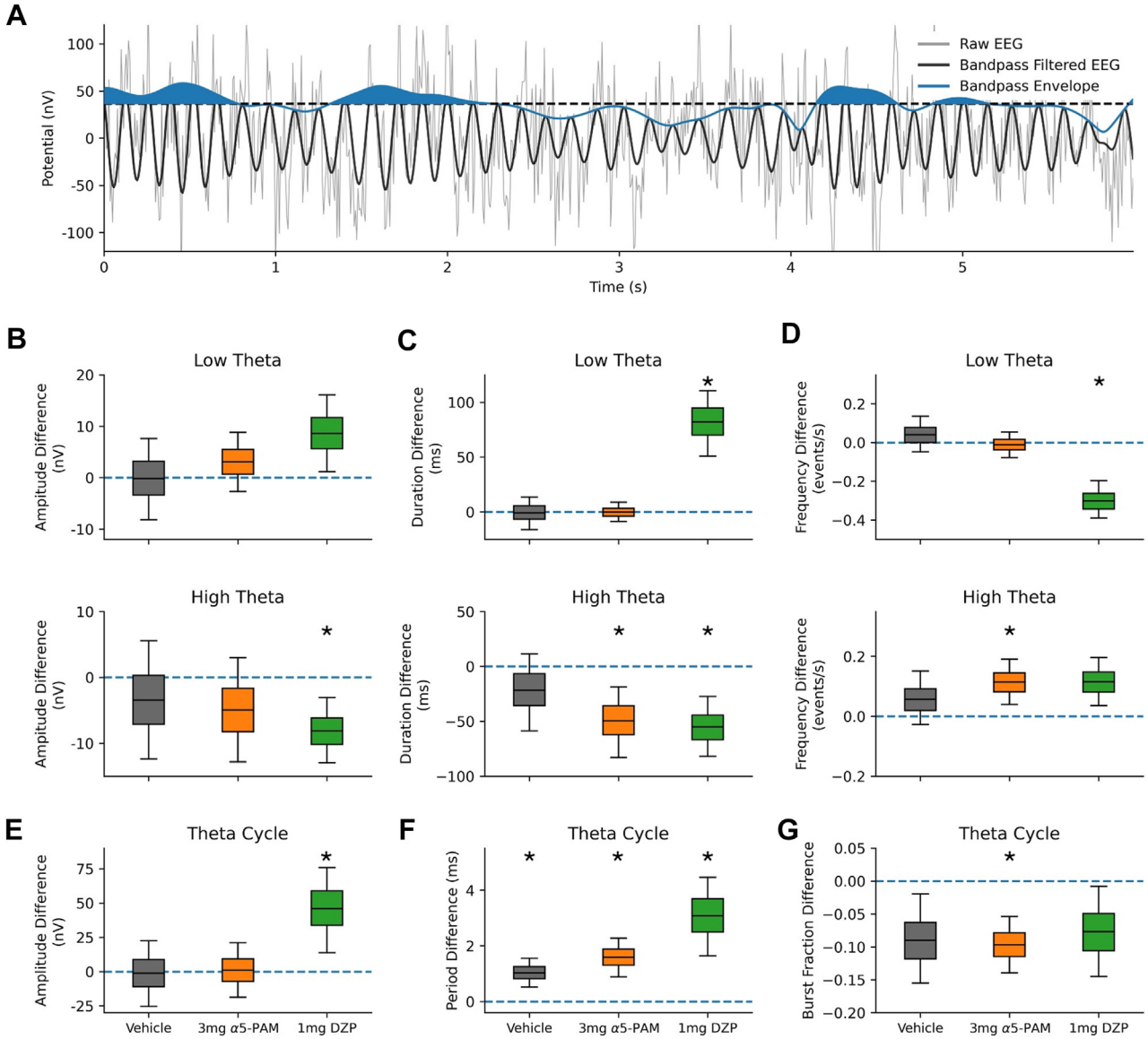

Figure 4. Signatures of α5-PAM and DZP in EEG waveform events. **(A)** Example trace of raw EEG waveform (gray), its high theta bandpass transformation (black), and instantaneous envelope (blue). The shaded blue area represents periods of theta events (elevated high-theta amplitude). The horizontal dotted line is the threshold for a large-amplitude event. **(B)** Event amplitude in different conditions for low-theta (top) and high-theta (bottom) bandpass-filtered EEG. **(C)** Same as panel **(B)** but for event duration. **(D)** Same as panel **(B)** but for event frequency. **(E–G)** Cycle-by-cycle difference in theta (3–9 Hz) amplitude **(E)**, period **(F)**, or burst fraction **(G)**. Error bars show the bootstrapped mean difference from baseline and 95% CI. α5-PAM, α5-$GABA_A$ receptor subunit positive allosteric modulator; DZP, diazepam; EEG, electroencephalography.

interneurons modulate theta power during both task and at rest support the possibility of α5-PAM EEG signatures for additional states. Future investigations may benefit from larger sample size to improve the characterization of α5-PAM effects, e.g., to investigate whether a slight increase in alpha power that was seen in a single rat in our study indicates a possible alpha power increase or sharper theta oscillation. Relatedly, a larger sample size will allow for further state-specific signatures of α5-PAM in EEG. Future studies should also include exposure data to better characterize GL-II-73 and EEG changes, such as associated brain and plasma levels and receptor occupancy. Finally, future work should characterize the EEG signatures of α5-PAM in stressed rats to relate the antidepressant effects of α5-PAM to EEG biomarkers.

Conclusions

To our knowledge, this is the first study to identify EEG signatures of α5-PAM ligand GL-II-73, which has previously been shown to have antidepressant, procognitive, and anxiolytic effects in preclinical tests in chronically stressed rodents (8). The EEG signatures can serve as biomarkers for noninvasive monitoring of α5-PAM treatment in preclinical testing to facilitate translation of the pharmacology to human trials. The similarity to EEG changes in depression indicate that the EEG

biomarkers that we characterized will be also relevant to monitoring pharmacology efficacy in humans.

ACKNOWLEDGMENTS AND DISCLOSURES

FM, AG-M, and EH thank the Krembil Foundation for their generous funding support. FM was also supported by an Ontario Graduate Scholarship.

FM was responsible for analysis of the data. FM, AG-M, TDP, TV, ES, and EH were responsible for interpretation of the data. FM and EH were responsible for manuscript drafting. FM, EH, TDP, and ES were responsible for manuscript revisions critically for important intellectual content. FM, EH, TDP, and ES were responsible for manuscript final approval. FM and EH were responsible for work accountability.

A previous version of this article was published as a preprint on bioRxiv: https://doi.org/10.1101/2024.03.26.586837.

ES and TDP are listed inventors on patents covering syntheses and use of α5-PAM compounds (Title: Treatment of Cognitive and mood systems in Neurodegenerative and Neuropsychiatric disorders with alpha 5—containing $GABA_A$ selective agonist, U.S., Canada, EU, JP, Australia, 62/310,409; Title: Compositions And Methods Relating To Use Of Agonists Of Alpha5- Containing $GABA_A$ Receptors, U.S., Canada, EU, JP, Australia, 62/805,009; Title: Imidazobenzodiazepines for treatment of cognitive and mood symptoms, U.S., Canada, EU, JP, Australia, PCT/US2022/042832). EH, ES, and TDP are listed inventors, and AG-M, FM, and TV are listed as collaborators on a patent covering in silico EEG biomarkers for monitoring α5-PAM treatment efficacy (Title: EEG biomarkers for Alpha5-PAM therapy, United States, 63/382,577). ES is the Founder and Board Member and TDP is the Director of Operations of Damona Pharmaceuticals, a biopharma dedicated to bringing α5-PAM compounds to the clinic.

ARTICLE INFORMATION

From the Krembil Centre for Neuroinformatics, Centre for Addiction and Mental Health, Toronto, Ontario, Canada (FM, AG-M, EH); Department of Physiology, University of Toronto, Toronto, Ontario, Canada (FM, EH); Department of Psychiatry, University of Toronto, Toronto, Ontario, Canada (TDP, ES, EH); Campbell Family Mental Health Research Institute, Centre for Addiction and Mental Health, Toronto, Ontario, Canada (TDP, ES); Krembil Brain Institute, University Healthy Network, Toronto, Ontario, Canada (TV); Department of Electrical and Computer Engineering, University of Toronto, Toronto, Ontario, Canada (TV); Institute of Biomaterials and Biomedical Engineering, University of Toronto, Toronto, Ontario, Canada (TV); Department of Surgery, University of Toronto, Toronto, Ontario, Canada (TV), Center for Advancing Neurotechnological Innovation to Application, Toronto, Ontario, Canada (TV); Max Planck-University of Toronto Center for Neural Science and Technology, Toronto, Ontario, Canada (TV); Institute of Medical Sciences, University of Toronto, Toronto, Ontario, Canada (TV); and Department of Pharmacology & Toxicology, University of Toronto, Toronto, Ontario, Canada (ES).

Address correspondence to Etay Hay, Ph.D., at etay.hay@camh.ca.

Received Jun 28, 2024; revised Nov 18, 2024; accepted Dec 11, 2024.

Supplementary material cited in this article is available online at https://doi.org/10.1016/j.bpsgos.2024.100435.

REFERENCES

1. Lin LC, Sibille E (2015): Somatostatin, neuronal vulnerability and behavioral emotionality. Mol Psychiatry 20:377–387.
2. Luscher B, Shen Q, Sahir N (2011): The GABAergic deficit hypothesis of major depressive disorder. Mol Psychiatry 16:383–406.
3. Nemeroff CB (2003): The role of GABA in the pathophysiology and treatment of anxiety disorders. Psychopharmacol Bull 37:133–146.
4. Gavilán MP, Revilla E, Pintado C, Castaño A, Vizuete ML, Moreno-González I, *et al.* (2007): Molecular and cellular characterization of the age-related neuroinflammatory processes occurring in normal rat hippocampus: Potential relation with the loss of somatostatin GABAergic neurons. J Neurochem 103:984–996.
5. Fuhrer TE, Palpagama TH, Waldvogel HJ, Synek BJL, Turner C, Faull RL, Kwakowsky A (2017): Impaired expression of GABA transporters in the human Alzheimer's disease hippocampus, subiculum, entorhinal cortex and superior temporal gyrus. Neuroscience 351:108–118.
6. Edinoff AN, Nix CA, Hollier J, Sagrera CE, Delacroix BM, Abubakar T, *et al.* (2021): Benzodiazepines: Uses, dangers, and clinical considerations. Neurol Int 13:594–607.
7. Sigel E, Ernst M (2018): The benzodiazepine binding sites of GABAA receptors. Trends Pharmacol Sci 39:659–671.
8. Prevot TD, Li G, Vidojevic A, Misquitta KA, Fee C, Santrac A, *et al.* (2019): Novel benzodiazepine-like ligands with various anxiolytic, antidepressant, or pro-cognitive profiles. Mol Neuropsychiatry 5:84–97.
9. Piantadosi SC, French BJ, Poe MM, Timić T, Marković BD, Pabba M, *et al.* (2016): Sex-dependent anti-stress effect of an α5 subunit containing $GABA_A$ receptor positive allosteric modulator. Front Pharmacol 7:446.
10. Smith KS, Engin E, Meloni EG, Rudolph U (2012): Benzodiazepine-induced anxiolysis and reduction of conditioned fear are mediated by distinct $GABA_A$ receptor subtypes in mice. Neuropharmacology 63:250–258.
11. Behlke LM, Foster RA, Liu J, Benke D, Benham RS, Nathanson AJ, *et al.* (2016): A pharmacogenetic "restriction-of-function" approach reveals evidence for anxiolytic-like actions mediated by α5-containing $GABA_A$ receptors in mice. Neuropsychopharmacology 41:2492–2501.
12. Botta P, Demmou L, Kasugai Y, Markovic M, Xu C, Fadok JP, *et al.* (2015): Regulating anxiety with extrasynaptic inhibition. Nat Neurosci 18:1493–1500.
13. Koh MT, Rosenzweig-Lipson S, Gallagher M (2013): Selective GABA(A) α5 positive allosteric modulators improve cognitive function in aged rats with memory impairment. Neuropharmacology 64:145–152.
14. Bettler B, Kaupmann K, Mosbacher J, Gassmann M (2004): Molecular structure and physiological functions of GABA(B) receptors. Physiol Rev 84:835–867.
15. Möhler H (2006): GABA(A) receptor diversity and pharmacology. Cell Tissue Res 326:505–516.
16. Jacob TC (2019): Neurobiology and therapeutic potential of α5-GABA type A receptors. Front Mol Neurosci 12:179.
17. Nutt D (2006): GABAA receptors: Subtypes, regional distribution, and function. J Clin Sleep Med 2:S7–S11.
18. Pirker S, Schwarzer C, Wieselthaler A, Sieghart W, Sperk G (2000): $GABA_A$ receptors: Immunocytochemical distribution of 13 subunits in the adult rat brain. Neuroscience 101:815–850.
19. Ghafari M, Falsafi SK, Szodorai E, Kim E-J, Li L, Höger H, *et al.* (2017): Formation of $GABA_A$ receptor complexes containing α1 and α5 subunits is paralleling a multiple T-maze learning task in mice. Brain Struct Funct 222:549–561.
20. Prenosil GA, Schneider Gasser EM, Rudolph U, Keist R, Fritschy J-M, Vogt KE (2006): Specific subtypes of $GABA_A$ receptors mediate phasic and tonic forms of inhibition in hippocampal pyramidal neurons. J Neurophysiol 96:846–857.
21. Glykys J, Mody I (2006): Hippocampal network hyperactivity after selective reduction of tonic inhibition in $GABA_A$ receptor α5 subunit–deficient mice. J Neurophysiol 95:2796–2807.
22. Olsen RW, Sieghart W (2009): GABA A receptors: Subtypes provide diversity of function and pharmacology. Neuropharmacology 56:141–148.
23. Schulz JM, Knoflach F, Hernandez M-C, Bischofberger J (2018): Dendrite-targeting interneurons control synaptic NMDA-receptor activation via nonlinear α5-$GABA_A$ receptors. Nat Commun 9:3576.
24. Fuchs T, Jefferson SJ, Hooper A, Yee PH, Maguire J, Luscher B (2017): Disinhibition of somatostatin-positive GABAergic interneurons results in an anxiolytic and antidepressant-like brain state. Mol Psychiatry 22:920–930.
25. Martin LJ, Bonin RP, Orser BA (2009): The physiological properties and therapeutic potential of α5-$GABA_A$ receptors. Biochem Soc Trans 37:1334–1337.
26. Yao HK, Guet-McCreight A, Mazza F, Moradi Chameh H, Prevot TD, Griffiths JD, *et al.* (2022): Reduced inhibition in depression impairs stimulus processing in human cortical microcircuits. Cell Rep 38:110232.
27. Mazza F, Guet-McCreight A, Valiante TA, Griffiths JD, Hay E (2023): In-silico EEG biomarkers of reduced inhibition in human cortical microcircuits in depression. PLoS Comput Biol 19:e1010986.
28. Crestani F, Keist R, Fritschy JM, Benke D, Vogt K, Prut L, *et al.* (2002): Trace fear conditioning involves hippocampal α5 $GABA_A$ receptors. Proc Natl Acad Sci U S A 99:8980–8985.

29. Collinson N, Kuenzi FM, Jarolimek W, Maubach KA, Cothliff R, Sur C, *et al.* (2002): Enhanced learning and memory and altered GABAergic synaptic transmission in mice lacking the alpha 5 subunit of the $GABA_A$ receptor. J Neurosci 22:5572–5580.
30. Zurek AA, Kemp SWP, Aga Z, Walker S, Milenkovic M, Ramsey AJ, *et al.* (2016): α5$GABA_A$ receptor deficiency causes autism-like behaviors. Ann Clin Transl Neurol 3:392–398.
31. Fee C, Prevot TD, Misquitta K, Knutson DE, Li G, Mondal P, *et al.* (2021): Behavioral deficits induced by somatostatin-positive GABA neuron silencing are rescued by alpha 5 GABA-A receptor potentiation. Int J Neuropsychopharmacol 24:505–518.
32. Thio BJ, Grill WM (2023): Relative contributions of different neural sources to the EEG. NeuroImage 275:120179.
33. van Lier H, Drinkenburg WHIM, van Eeten YJW, Coenen AML (2004): Effects of diazepam and zolpidem on EEG beta frequencies are behavior-specific in rats. Neuropharmacology 47:163–174.
34. Mikulovic S, Restrepo CE, Siwani S, Bauer P, Pupe S, Tort ABL, *et al.* (2018): Ventral hippocampal OLM cells control type 2 theta oscillations and response to predator odor. Nat Commun 9:3638.
35. Martin LJ, Zurek AA, MacDonald JF, Roder JC, Jackson MF, Orser BA (2010): Alpha5$GABA_A$ receptor activity sets the threshold for long-term potentiation and constrains hippocampus-dependent memory. J Neurosci 30:5269–5282.
36. Chung H, Park K, Jang HJ, Kohl MM, Kwag J (2020): Dissociation of somatostatin and parvalbumin interneurons circuit dysfunctions underlying hippocampal theta and gamma oscillations impaired by amyloid β oligomers in vivo. Brain Struct Funct 225:935–954.
37. Skinner FK, Rich S, Lunyov AR, Lefebvre J, Chatzikalymniou AP (2021): A hypothesis for theta rhythm frequency control in CA1 microcircuits. Front Neural Circuits 15:643360.
38. Kragel JE, VanHaerents S, Templer JW, Schuele S, Rosenow JM, Nilakantan AS, Bridge DJ (2020): Hippocampal theta coordinates memory processing during visual exploration. eLife 9:e52108.
39. Donoghue T, Haller M, Peterson EJ, Varma P, Sebastian P, Gao R, *et al.* (2020): Parameterizing neural power spectra into periodic and aperiodic components. Nat Neurosci 23:1655–1665.
40. Cole S, Voytek B (2019): Cycle-by-cycle analysis of neural oscillations. J Neurophysiol 122:849–861.
41. Antsiperov VE, Obukhov YuV, Komol'tsev IG, Gulyaeva NV (2017): Segmentation of quasiperiodic patterns in EEG recordings for analysis of post-traumatic paroxysmal activity in rat brains. Pattern Recognit Image Anal 27:789–803.
42. Kadam SD, D'Ambrosio R, Duveau V, Roucard C, Garcia-Cairasco N, Ikeda A, *et al.* (2017): Methodological standards and interpretation of video-electroencephalography in adult control rodents. A TASK1-WG1 report of the AES/ILAE Translational Task Force of the ILAE. Epilepsia 58(suppl 4):10–27.
43. Newson JJ, Thiagarajan TC (2018): EEG frequency bands in psychiatric disorders: A review of resting state studies. Front Hum Neurosci 12:521.
44. Xiao J, Provenza NR, Asfouri J, Myers J, Mathura RK, Metzger B, *et al.* (2023): Decoding depression severity from intracranial neural activity. Biol Psychiatry 94:445–453.
45. Fernández-Palleiro P, Rivera-Baltanás T, Rodrigues-Amorim D, Fernández-Gil S, del Carmen Vallejo-Curto M, Álvarez-Ariza M, *et al.* (2020): Brainwaves oscillations as a potential biomarker for major depression disorder risk. Clin EEG Neurosci 51:3–9.
46. Arns M, Etkin A, Hegerl U, Williams LM, DeBattista C, Palmer DM, *et al.* (2015): Frontal and rostral anterior cingulate (rACC) theta EEG in depression: Implications for treatment outcome? Eur Neuropsychopharmacol 25:1190–1200.
47. Jaworska N, Blier P, Fusee W, Knott V (2012): Alpha power, alpha asymmetry and anterior cingulate cortex activity in depressed males and females. J Psychiatr Res 46:1483–1491.
48. Grin-Yatsenko VA, Baas I, Ponomarev VA, Kropotov JD (2010): Independent component approach to the analysis of EEG recordings at early stages of depressive disorders. Clin Neurophysiol 121:281–289.
49. Bailey NW, Hoy KE, Rogasch NC, Thomson RH, McQueen S, Elliot D, *et al.* (2018): Responders to rTMS for depression show increased fronto-midline theta and theta connectivity compared to non-responders. Brain Stimul 11:190–203.
50. Bruder GE, Sedoruk JP, Stewart JW, McGrath PJ, Quitkin FM, Tenke CE (2008): Electroencephalographic alpha measures predict therapeutic response to a selective serotonin reuptake inhibitor antidepressant: Pre- and post-treatment findings. Biol Psychiatry 63:1171–1177.
51. Peng Z, Zhou C, Xue S, Bai J, Yu S, Li X, *et al.* (2018): Mechanism of repetitive transcranial magnetic stimulation for depression. Shanghai Arch Psychiatry 30:84–92.
52. Downar J, Daskalakis ZJ (2013): New targets for rTMS in depression: A review of convergent evidence. Brain Stimul 6:231–240.
53. Murphy SC, Palmer LM, Nyffeler T, Müri RM, Larkum ME (2016): Transcranial magnetic stimulation (TMS) inhibits cortical dendrites. eLife 5:e13598.
54. Paus T, Barrett J (2004): Transcranial magnetic stimulation (TMS) of the human frontal cortex: Implications for repetitive TMS treatment of depression. J Psychiatry Neurosci 29:268–279.
55. Meghdadi AH, Stevanović Karić M, McConnell M, Rupp G, Richard C, Hamilton J, *et al.* (2021): Resting state EEG biomarkers of cognitive decline associated with Alzheimer's disease and mild cognitive impairment. PLoS One 16:e0244180.
56. Xing M, Tadayonnejad R, MacNamara A, Ajilore O, DiGangi J, Phan KL, *et al.* (2017): Resting-state theta band connectivity and graph analysis in generalized social anxiety disorder. NeuroImage Clin 13:24–32.
57. Northoff G, Sibille E (2014): Why are cortical GABA neurons relevant to internal focus in depression? A cross-level model linking cellular, biochemical and neural network findings. Mol Psychiatry 19:966–977.
58. Fee C, Banasr M, Sibille E (2017): Somatostatin-positive gamma-aminobutyric acid interneuron deficits in depression: cortical microcircuit and therapeutic perspectives. Biol Psychiatry 82:549–559.
59. Seney ML, Tripp A, McCune S, Lewis DA, Sibille E (2015): Laminar and cellular analyses of reduced somatostatin gene expression in the subgenual anterior cingulate cortex in major depression. Neurobiol Dis 73:213–219.
60. Fanselow EE, Richardson KA, Connors BW (2008): Selective, state-dependent activation of somatostatin-expressing inhibitory interneurons in mouse neocortex. J Neurophysiol 100:2640–2652.
61. Abbas AI, Sundiang MJM, Henoch B, Morton MP, Bolkan SS, Park AJ, *et al.* (2018): Somatostatin interneurons facilitate hippocampal-prefrontal synchrony and prefrontal spatial encoding. Neuron 100:926–939.e3.
62. Maheshwari A (2020): Rodent EEG: Expanding the spectrum of analysis. Epilepsy Curr 20:149–153.
63. Watrous AJ, Deuker L, Fell J, Axmacher N (2015): Phase-amplitude coupling supports phase coding in human ECoG. eLife 4:e07886.
64. Wirt RA, Crew LA, Ortiz AA, McNeela AM, Flores E, Kinney JW, Hyman JM (2021): Altered theta rhythm and hippocampal-cortical interactions underlie working memory deficits in a hyperglycemia risk factor model of Alzheimer's disease. Commun Biol 4:1–16.
65. Jones MW, Wilson MA (2005): Theta rhythms coordinate hippocampal-prefrontal interactions in a spatial memory task. PLoS Biol 3:e402.
66. Christian EP, Snyder DH, Song W, Gurley DA, Smolka J, Maier DL, *et al.* (2015): EEG-β/γ spectral power elevation in rat: A translatable biomarker elicited by GABA(Aα2/3)-positive allosteric modulators at nonsedating anxiolytic doses. J Neurophysiol 113:116–131.
67. Reeves-Darby JA, Berro LF, Platt DM, Rüedi-Bettschen D, Shaffery JP, Rowlett JK (2023): Pharmaco-EEG analysis of ligands varying in selectivity for α1 subunit-containing $GABA_A$ receptors during the active phase in rats. Psychopharmacol (Berl) 240:2561–2571.
68. Acharya JN, Acharya VJ (2019): Overview of EEG montages and principles of localization. J Clin Neurophysiol 36:325–329.
69. Silberberg G, Markram H (2007): Disynaptic inhibition between neocortical pyramidal cells mediated by Martinotti cells. Neuron 53:735–746.
70. Huang P, Xiang X, Chen X, Li H (2020): Somatostatin neurons govern theta oscillations induced by salient visual signals. Cell Rep 33: 108415.
71. Funk CM, Peelman K, Bellesi M, Marshall W, Cirelli C, Tononi G (2017): Role of somatostatin-positive cortical interneurons in the generation of sleep slow waves. J Neurosci 37:9132–9148.